Solar Energy Materials and Solar Cells 184 (2018) 38–47

Contents lists available at ScienceDirect

Solar Energy Materials and Solar Cells

journal homepage: www.elsevier.com/locate/solmat

# Carrier population control and surface passivation in solar cells

Andres Cuevas[a,*], Yimao Wan[a], Di Yan[a], Christian Samundsett[a], Thomas Allen[b], Xinyu Zhang[c], Jie Cui[d], James Bullock[e]

[a] Research School of Engineering, The Australian National University, Canberra 2601, Australia
[b] King Abdullah University of Science and Technology (KAUST), KAUST Solar Center (KSC), Thuwal 23955-6900, Saudi Arabia
[c] R&D Centre, Jinko Solar Co., Ltd., Haining 314400, China
[d] The Boston Consulting Group, 161 Castlereagh Street, Sydney, NSW 2000, Australia
[e] Department of Electrical Engineering and Computer Sciences, University of California, Berkeley, CA 94720, USA

ARTICLE INFO

*Keywords:*
Surface passivation
Carrier-selective contacts
Silicon solar cells

ABSTRACT

Controlling the concentration of charge carriers near the surface is essential for solar cells. It permits to form regions with selective conductivity for either electrons or holes and it also helps to reduce the rate at which they recombine. Chemical passivation of the surfaces is equally important, and it can be combined with population control to implement carrier-selective, passivating contacts for solar cells. This paper discusses different approaches to suppress surface recombination and to manipulate the concentration of carriers by means of doping, work function and charge. It also describes some of the many surface-passivating contacts that are being developed for silicon solar cells, restricted to experiments performed by the authors.

## 1. Introduction

Maintaining a high concentration of electrons and holes in a photon-absorbing semiconductor is a premise for the conceptual design of a solar cell. This is because the electrochemical energy of electrons and holes is directly linked to their concentration, and so is the eventual voltage produced by the device. Although they may be referred to as a gas, simplifying the statistical relationships that govern their population density, electrons and holes do not leak out of the surfaces of the semiconductor; rather, they recombine with each other at surface defects, with the same net effect of being lost and of causing a reduction of the electrochemical energy of the system. Hence, it is important to envelop the semiconductor absorber with a "skin" that passivates those surface defects [1]. Intuitively, passivation can be envisaged as the covalent bonding between atoms present in the "skin" material and the surface atoms of the semiconductor. An example is the bonding between oxygen and silicon that results from thermally growing a $SiO_2$ layer. The oxidation process still leaves a fraction of silicon bonds unsatisfied and it is usually complemented by supplying hydrogen, whose small size facilitates its diffusion towards those dangling silicon bonds.

While the concept of chemical passivation is intuitively clear and widely accepted, the term "passivation" is sometimes used to refer to other mechanisms that also result in a reduction of the recombination rate between electrons and holes. Generally, such mechanisms involve a large imbalance between the populations of electrons and holes near the surface, which indeed leads to a lower recombination rate, as described below. To preserve the intuitive meaning of passivation as chemical bonding, we will refer to other, non-chemical mechanisms as "carrier population control".

Another premise for a semiconductor absorber to become a solar cell is that it should be able to deliver electrons to an external circuit. For that to occur, each carrier type must flow separately towards each of the two metallic terminals attached to the solar cell. This implies that each of those metallic terminals must be in contact with a region in the semiconductor where the conductivity for one carrier type is much greater than for the other carrier type [2]. Those two regions could be appropriately called selective electron and hole conductors, but given that they need to be at the surface and in contact with the metal terminals, they are frequently referred to as selective contacts.

The ability to manipulate the conductivity is, therefore, essential to construct a solar cell. Of the two components that determine the conductivity, mobility and charge carrier concentration, only the latter can be varied to a sufficient extent in practice. In silicon technology that is usually achieved by doping, but other methods can be used, for instance by depositing materials with a work function significantly higher or lower than that of the silicon absorber, as discussed in this paper.

The conceptual premises are clear, but their experimental implementation can be challenging. Metallic terminals are essential, but when a metal is directly deposited on silicon it causes a very high density of recombination centres, which draws to the surface both carrier types, thus undermining the objective of achieving single-carrier transport. Hence, it is important to find ways of implementing a highly

* Corresponding author.

https://doi.org/10.1016/j.solmat.2018.04.026
Received 15 February 2018; Received in revised form 6 April 2018; Accepted 23 April 2018

asymmetric conductivity to each of the two metallic terminals while minimising recombination. In conventional silicon solar cells surface passivation and selective conductivity are implemented “in parallel”, which leaves the surface regions contacted by the metallic terminals depassivated. An awareness of the limitations that recombination at the metal contacts cause has prompted the development of comprehensive contact systems where selective conductivity and surface passivation are implemented “in series”. Indeed, the most effective contact systems developed so far combine several layers of different materials, each of them performing one of the required functions of selective conduction, surface passivation and contact formation to the external metal.

This paper summarises the main results of our work during the last five years on non-traditional surface passivating materials and carrier-selective passivating contacts. Please note that a substantial part of that work has been in collaboration with other researchers, as mentioned in the Acknowledgement. Given that this paper is intended for a special issue on surface passivation and passivating contacts, no attempt has been made to include the outstanding work done by other researchers on those topics, in order to avoid excessive repetition. It is expected that companion articles of the same issue will give the interested reader a more comprehensive overview of the topic.

## 2. Pathways to reduce surface recombination

### 2.1. Surface passivation by chemical bonding

Surface passivation refers, in its purest form, to the chemical attachment of atomic or molecular species to the unsatisfied “dangling” bonds of silicon atoms at the surface of the semiconductor. Usually, a certain amount of interface defects remains after an oxidation process or after depositing a dielectric material on a silicon wafer. The density of such defects, or traps $D_{it}$ can be drastically reduced by means of a hydrogenation treatment. For example, Eades et al. measured $D_{it} \sim 10^9$ $cm^{-2}$ for *alnealed* $SiO_2$ [3], a remarkably low number in comparison with the $\sim 7 \times 10^{14}$ $cm^{-2}$ density of bonds present at the (100) silicon surface. The application of a hydrogenation treatment, preferably in atomic form, is a common denominator of all the approaches that have led to high quality surface passivation, including semiconductors, like a-Si: H, and dielectrics like $SiO_2$, $SiN_x$, $Al_2O_3$, $Ga_2O_3$, etc. For some of them it is difficult to measure accurately the density of interface traps, due to their non-negligible conductivity. This obviously applies to materials that are attractive for selective contact systems precisely because they are conductive. Fig. 1, updated from the original version in [4], gives a qualitative summary of the approximate levels of $D_{it}$ and fixed charge reported for a variety of passivating films, reflecting the substantial spread of the values reported in the literature. Note that this $D_{it}$ corresponds to the middle of the energy bandgap of silicon and, although useful to compare the quality of chemical passivation by different materials, it should only be regarded as a proxy for the complex statistics of Shockley-Read-Hall recombination.

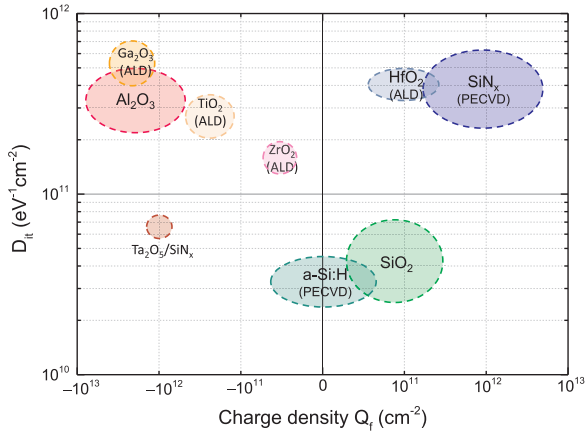


**Fig. 1.** Qualitative summary of the approximate ranges for the density of interface defects and the charge measured experimentally for different materials deposited on the surface of crystalline silicon. The vertical axis indicates the level of chemical passivation, whereas the horizontal axis indicates the ability of charge (both polarities) to assist in controlling the carrier density at the interface.

### 2.2. Controlling the population of electrons and holes by means of doping

The product of the concentrations of electrons and holes drives the rate at which they recombine. It is intuitive to understand that this reaction rate is highest when the concentration of the two reactants is similar to each other. Therefore, it is possible to control electron-hole recombination by manipulating their respective concentrations, basically, by making one of the two much smaller than the other. To illustrate that, let us consider SRH recombination in silicon caused by a relatively high density of mid-gap defects. It is straightforward to calculate the net recombination rate for any combination of dopant densities in the semiconductor using the well-known SRH expression, plus the relationship between the *pn* product and the difference between the electron and hole Fermi energies $E_{Fn}$ and $E_{Fp}$,

$$(p_o + \Delta p)(n_o + \Delta n) = n_i^2 \exp\left(\frac{E_{Fn} - E_{Fp}}{kT}\right) \quad (1)$$

where $p_0$ and $n_0$ are the equilibrium hole and electron concentrations, $\Delta p = \Delta n$ their respective excess concentrations under illumination, $n_i$ the intrinsic carrier density, $k$ the Boltzmann constant and $T$ the temperature. In a moderately doped p-type semiconductor $p_0 \approx N_A$ and $n_0 \approx n_i^2/N_A$, where $N_A$ is the concentration of acceptors. Fixing the difference $(E_{Fn}\text{-}E_{Fp})/q$ to a particular level, for example 600 mV allows us to determine the excess carrier concentration and, eventually, the recombination rate when we change the dopant concentration in the semiconductor. Fig. 2 shows the recombination rate as a function of the ratio between the electron and hole concentrations for two different recombination centres, one that presents a capture cross-section for electrons 100 times greater than for holes (k = $\sigma_n/\sigma_p$ = 100) and

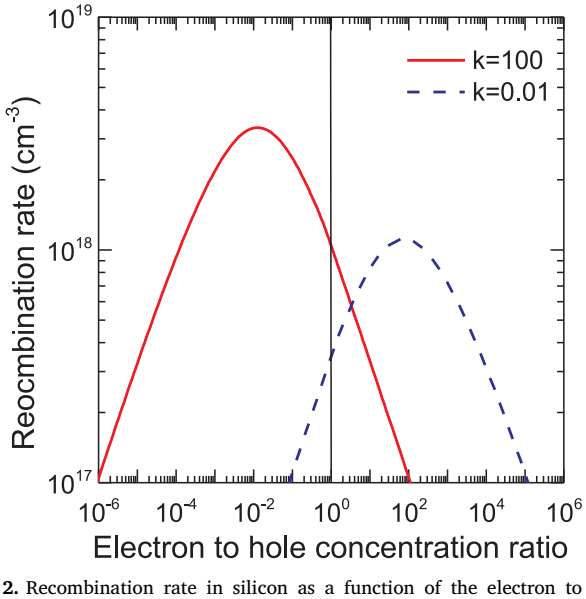


**Fig. 2.** Recombination rate in silicon as a function of the electron to hole concentration ratio for a fixed separation between the electron and hole quasi-Fermi energies of 0.6 V. The two cases shown correspond to recombination centres with a capture cross-section for electrons ($\sigma_n = 10^{-13}$ $cm^{-2}$) 100 times greater than for holes (k = 100) or 100 times smaller (k = 0.01, $\sigma_n = 10^{-15}$ $cm^{-2}$). A density of defects 3 times lower for the second defect ($N_{t2} = 3 \times 10^{10}$ $cm^{-3}$) has been assumed.

another one where it is 100 times smaller (k = 0.01). We have assumed two mid-gap defects, with a density three times greater for the first ($N_t = 9 \times 10^{10}$ cm$^{-3}$) than the second. As expected, the maximum recombination rate occurs when $n\sigma_n \approx p\sigma_p$. For a defect with identical capture cross sections for electrons and holes the recombination rate is highest when $p = n$. Although the calculations presented in Fig. 2 are simplistic, they are qualitatively similar to the measurements reported by Yablonovitch et al. [5] for the interface between thermal $SiO_2$ and Si. In general, increasing the majority carrier concentration brings about a reduction of the minority carriers and the overall recombination rate. Therefore, to reduce recombination, the equilibrium carrier concentrations need to be very asymmetric, by eight or ten orders of magnitude ($n_0/p_0 < 10^{-8}$ cm$^2$), so that such asymmetry remains under excitation.

That doping can be used to reduce the impact of surface recombination can be and has been verified experimentally. For example, the effective carrier lifetime that can be measured in an unpassivated silicon wafer is in the range of 1–3 μs, depending on the thickness of the wafer and the diffusivity of the relevant minority carrier. When a dopant diffusion is added near the surfaces of the wafer, the effective lifetime increases to tens or even hundreds of μs. It is possible to reduce recombination even without an outer dielectric coating [6], but it is of course more complete with it. The ability of a diffused region to suppress recombination is compromised by recombination within its own volume; this is because although dopant diffusions are quite thin, the concentration of one of the two charge carriers is very high, which triggers the Auger process, leading to fast recombination of the minority carriers. Globally, recombination within the volume of the diffused region and at the outer surface can be encapsulated in a "recombination parameter" with dimensions of current density, $J_0$, that is easily measurable using the method proposed by Kane and Swanson [7]. It is possible to translate such $J_0$ parameter into an equivalent surface recombination velocity, and vice-versa.

### 2.3. Charge-assisted population control

Some insulators possess, or develop in contact with a silicon surface, a net positive or negative charge. In equilibrium, this has the consequence of attracting carriers having an opposite charge, which accumulate at the interface between the dielectric and the semiconductor. A common example is $SiN_x$, whose positive charge creates a very thin layer where the concentration of electrons is overwhelmingly greater than that of holes. For normal solar cell operation conditions (moderate illumination intensity), a large asymmetry between the concentrations of majority and minority carriers remains, which, as shown above, leads to a reduced recombination rate. Many people refer to this as "field effect passivation", but the root cause of the lower recombination rate is the asymmetric population of electrons and holes caused by the charge. As Würfel has explained [8], an electric field established in equilibrium cannot exert a force on the excess carriers generated by an external excitation.

A similar argument can be made for the case of a negative charge, which would create an induced layer where holes are in the majority and electrons in the minority. Irrespective of the bulk semiconductor being p-type or n-type, either an accumulation or an inversion layer have the consequence of altering the statistics of electron-hole recombination and, with some exceptions, they mitigate the influence of residual defects at the surface. The preference for a particular charge polarity may come from the knowledge of the capture cross-sections for electrons and holes of the dominant surface defects. More commonly the decision is made based on device structure considerations; for example, a positively charged dielectric like $SiN_x$, causes an inversion layer on p-type silicon, which then channels minority electrons towards highly defective regions, such as those at the edge of the device, or regions with a high recombination rate, such as those locally contacted to the external metallic terminal. Hence, to avoid the problem, a negatively charged dielectric like $Al_2O_3$ is commonly used to passivate the rear side of p-type Si solar cells with a localised metal contact.

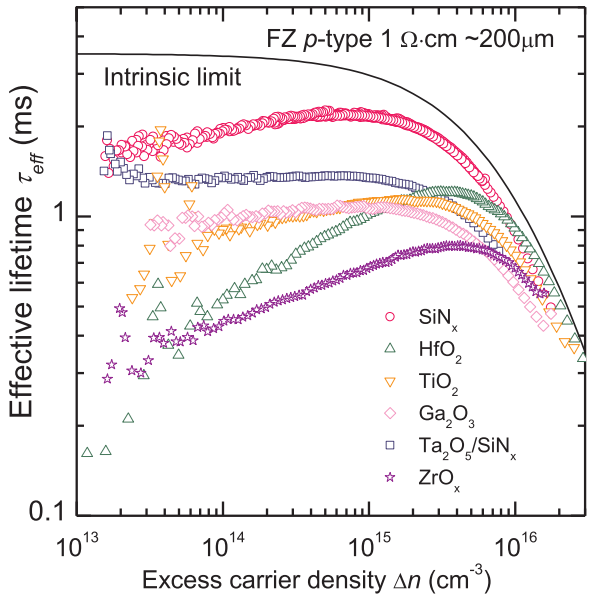


**Fig. 3.** Effective minority carrier lifetime measured for p-type silicon wafers with a resistivity of about 1 Ω cm coated on both sides with various metal oxides. A sample coated with SiNx is included as a reference.

Searching for alternatives to $Al_2O_3$, we have investigated other materials that could provide both a negative charge and effective chemical passivation (Fig. 3). To achieve the latter, we have used hydrogen containing precursors in an ALD reactor. Table 1 shows a varying level of negative charge, high for $Ga_2O_3$, and lower, but still significant, for $TiO_2$ and $Ta_2O_5$. For $HfO_2$ we found a slightly positive charge, although other researchers have reported a negative one. The case of $Ta_2O_5$ is interesting, since hydrogenation did not occur to a sufficient degree until a second layer of hydrogen-rich $SiN_x$ was deposited onto it and annealed; this shows that even a strong negative charge can be insufficient to reduce surface recombination. Capping with $SiN_x$ and subsequent annealing frequently enhances the quality of passivation provided by other materials too; for example, the surface recombination velocity measured for $GaO_x$ improved from 2.5 cm/s to 1.4 cm/s [9]. In addition, the well-known fact that high quality surface passivation can be achieved by a-Si:H or hydrogenated $SiO_2$, both of which have low or negligible charge density, indicates that chemical passivation can be effective even in the absence of carrier population control.

**Table 1**
Surface recombination parameters measured for various dielectric materials deposited on p-Si and n-Si wafers with a bulk resistivity of approximately 1–1.6 Ω cm, as well as onto boron or phosphorus diffused surfaces. The dopant diffusions had a Rsheet in the range of 85–120 Ω/□. The corresponding charge density, obtained from C-V measurements is also given.

| Material | $Q_{eff}/q$ ($10^{12}$ cm$^{-2}$) | $S_{eff}$ of undiffused wafers (cm/s) | | $J_0$ of dopant diffusions (fA/cm$^2$) | | Method/ Reference |
|---|---|---|---|---|---|---|
| | | *p*-type | *n*-type | $p^+$ | $n^+$ | |
| $SiN_x$ | + 0.6 | 1.6 | < 1.0 | | 44 | PECVD [10] |
| a-Si:H/$SiN_x$ | | 3.0 | 2.0 | 87 | 47 | PECVD [11] |
| $HfO_2$ | + 0.5 | 9.9 | 3.3 | | 23 | ALD [12,13] |
| $Ga_2O_3$ | − 5.0 | 2.5 | | 26 | | ALD [14] |
| $TiO_2$ | − 0.8 | 9.8 | 2.5 | 19 | | ALD [15] |
| $Ta_2O_5$/$SiN_x$ | − 1.0 | 5.0 | 3.2 | 25 | 68 | ALD/PECVD [16] |
| $ZrO_x$ | − 0.058 | 13.0 | 8.0 | | | ALD [17] |

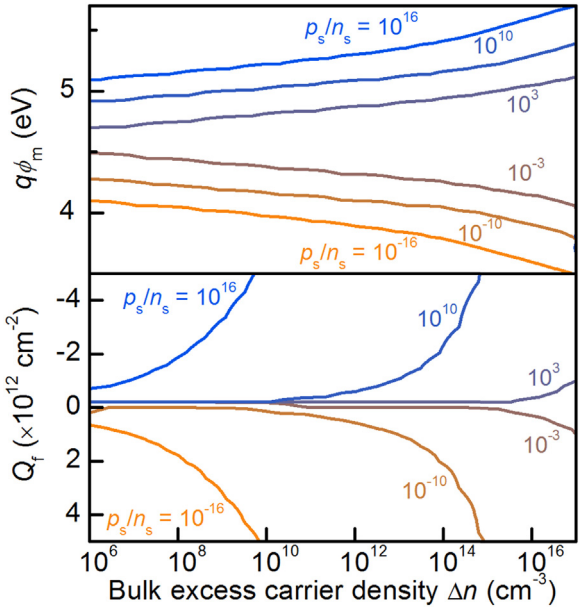


**Fig. 4.** Surface hole to electron concentration ratio $p_s/n_s$ calculated as a function of the excess carrier density in the bulk of a lowly doped ($N_D = 10^{14}$ cm$^{-3}$) n-type *c*-Si wafer with an applied work function (top) or fixed charge density (bottom). Figure from J. Bullock, PhD thesis, The Australian National University, 2016.

### 2.4. Work-function control

According to the ideal Schottky-Mott theory, a difference between the chemical potentials, or work functions, of the deposited material and the semiconductor can result in a high concentration of one type of carrier near the surface and, consequently, a low concentration of the other type. As mentioned above, this asymmetry in carrier concentrations can help to reduce the recombination rate. The concentration of electrons and holes at the surface $n_s$ and $p_s$ is calculated from the electrostatic potential at the surface of the semiconductor $\psi_s$, which can be found by solving the electrostatic equations following the iterative approach of Girisch et al. [18]. The surface potential $\psi_s$ is reduced when an excess concentration of carriers $\Delta n$ is present in the semiconductor. However, a large asymmetry in the surface carrier concentrations can still exist at one sun illumination if the initial $\psi_s$ is sufficiently large. Fig. 4 shows calculations of the ratio $p_s/n_s$ as a function of the work function $q\phi_m$ of materials deposited onto lowly doped n-type silicon ($N_D = 10^{14}$ cm$^{-3}$), assuming an ideal surface with zero recombination and no pinning of the Fermi level. Given that the excess carrier concentration in the semiconductor can vary widely depending on the electronic quality of the silicon wafer and also with the operating point of the solar cell, the calculations have been performed for a range of $\Delta n$. It can be observed that to maintain a strong predominance of holes over electrons of $p_s/n_s = 1 \times 10^{16}$ cm$^{-3}$ over the range of excess carrier densities typical of solar cell operation it is necessary to deposit a material with a work function of about 5–6 eV, even in the ideal case. Conversely, to achieve a strong predominance of electrons, with an asymmetry ratio of $p_s/n_s = 1 \times 10^{-16}$ cm$^{-3}$, it is necessary to deposit a material with a work function of about 3–4 eV.

Fig. 4 also shows similar calculations for the case of a fixed charge density $Q_f$. A negative (positive) charge does cause accumulation of holes (electrons) near the surface, but the asymmetry ratio varies markedly with the excess carrier density $\Delta n$ in the bulk of the wafer. For example, a negative charge of $Q_f = -2 \times 10^{12}$ cm$^{-2}$ results in $p_s/n_s = 10^{16}$ cm$^{-3}$ if $\Delta n$ is lower than $10^8$ cm$^{-3}$ but only about $p_s/n_s = 10^{10}$ cm$^{-3}$ if $\Delta n \approx 10^{14}$ cm$^{-3}$.

## 3. Combining surface passivation and carrier-selective conductivity

As mentioned in the introduction, it is clear that to support a high concentration of excess electrons and holes in the semiconductor and to separate them towards the two terminals of the solar cell it is essential to suppress recombination everywhere in the device. In particular, surface passivation should be incorporated into any electron or hole contact system, in order to make it more selective. The reason for this is that the fate of charge carriers (for example holes) that may flow into the contact structure designed to predominantly transport the other type of carriers (i.e. electrons) is to recombine.

Historically, chemical passivation from dielectrics has been incorporated to doped (hence asymmetrically conductive) regions of the silicon wafer in parallel. This is because dielectric materials are poor conductors and they need to be locally removed to make contact to the silicon with a metal. The dielectric is usually removed from just 1–5% of the surface area, but even such a small fraction of de-passivated dopant diffusion can represent the largest loss of the whole carrier-selective conductor system. This points out the importance of keeping under the metal terminals a layer (or layers) that permits the flow of current while passivating the surface of the silicon, that is, of incorporating chemical passivation and selective conduction “in series”. Below we describe different approaches to do that, but first let us discuss how to evaluate the quality of a given carrier-selective contact structure.

### 3.1. Performance parameters for carrier-selective contacts

It is straightforward to evaluate the ability of a carrier-selective contact structure to pass electric current by means of its contact resistivity $\rho_c$, an intuitive parameter that can be measured using well-known test structures and methods. On the other hand, the best way to evaluate the selectivity, that is, the ability to hinder the transport of one of the two carriers, is by assessing the recombination loss within the contact structure, including its interface with the metallic terminal. A suitable metric to evaluate recombination within a specific region of the device is the recombination current parameter $J_{0c}$, which can also be easily measured. The sub-index zero indicates that this would ideally be a recombination-generation current extrapolated to equilibrium conditions, whereas the second sub-index indicates that we are referring to contact structures. A simple way to combine in a single parameter the limitations imposed both by recombination and resistance is an ‘upper-limit’ voltage given by [19],

$$V_{UL} = \frac{kT}{q} ln\left(\frac{J_{ph}}{J_{0c}}\right) - J_{ph}\rho_c, \quad (2)$$

Although it would be desirable to do the calculation at the maximum power point, it varies from cell to cell. Hence we propose to evaluate $V_{UL}$ using a well-established reference value for the current, such as the photogenerated current $J_{ph} = 43.31$ mA/cm$^2$ calculated in Ref. [20] for an ideal silicon solar cell. The resulting upper limit voltage is, therefore, unattainable, and its calculation combines an open-circuit assumption to evaluate the cap imposed by recombination, together with a pessimistic evaluation of the voltage drop due to contact resistance. Nevertheless, it is precisely the assumption of these extreme conditions that makes its calculation robust, subject only to the specific $J_{0c}$ and $\rho_c$ parameters of the contact. It is, in fact, a suitable and easy to quantify metric to assess carrier-selectivity, and it remains relevant at the maximum power conditions. This is demonstrated in Fig. 5, where contours of $V_{UL}$ are overlayed on simulations of the achievable solar cell performance, showing near perfect alignment with the efficiency contours. The slight departure between the numerical simulation using Quokka [21] and the analytical calculation of $V_{UL}$ in the low $J_{0c}$ range arises from the influence of Auger recombination in the bulk of the

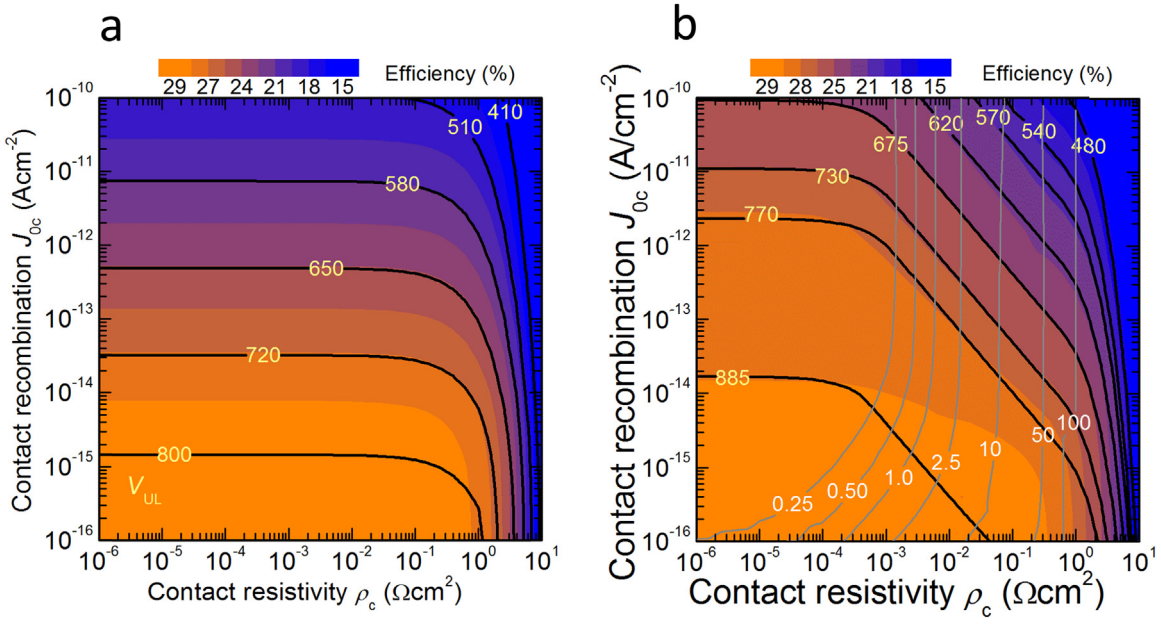


**Fig. 5.** (a) Comparison between the selectivity parameter $V_{UL}$ (black lines) and idealised simulations of solar cell performance using Quokka (colour contours), as a function of the rear contact $J_{0c}$ and $\rho_c$ for (a) a full area contact, or (b) a partial-area contact. In (b) the extra set of lines and lower numbers correspond to the optimum contact fraction. From J. Bullock, PhD thesis, The Australian National University, 2016. (For interpretation of the references to color in this figure legend, the reader is referred to the web version of this article).

wafer, which Eq. (2) does not account for, given that it is only possible to do that for every particular case (wafer thickness and doping).

Fig. 5(a) confirms the intuitive expectation that the influence of $\rho_c$ on a silicon solar cell with a full-area contact is minimal below $\sim 0.15\,\Omega\,cm^2$, whereas the impact of the recombination parameter $J_{0c}$ on cell voltage and efficiency is very strong. Nevertheless, there will be diminishing returns from reducing $J_{0c}$ below the limitations imposed by band to band and Auger recombination in the volume of the semiconductor absorber. For a 100 μm thick silicon wafer such limitation can be approximately established as $J_{0bulk} \approx 5 \times 10^{-15}$ A/cm$^2$, which imposes a limit to $V_{oc}$ of 761 mV [20].

Geometric restriction of the contact area provides an additional design tool to optimise the trade-off between recombination and resistance losses. Partial-area contacts can tolerate higher values of $J_{0c}$, but place greater demands on $\rho_c$, as well as creating more complexity in device fabrication. The $V_{UL}$ metric can be modified to approximately take into consideration the contact area,

$$V_{UL} = V_t ln\left(\frac{J_{ph}}{f_c J_{0c} + (1-f_c) J_{0pass}}\right) - J_{ph}\frac{\rho_c}{f_c} \quad (3)$$

where additional terms for the rear contact fraction $f_c$ and recombination in the non-contacted, surface passivated regions $J_{0pass}$ are included. Contour plots for the case of partial-area contacts, are shown in Fig. 5(b). A detailed description of the modelling assumptions, can be found in [19]. Similar calculations and graphs have been independently published by Brendel and Peibst. [22].

### 3.2. Combining dielectrics and doping "in parallel"

The benefits of applying a passivating dielectric to the front dopant diffusion of a silicon solar cell were first reported by Fossum and Burgess in 1978 [23]. They showed that the open-circuit voltage of a $p^+nn^+$ solar cell increased by 30 mV when a very thin (5 nm) $SiO_2$ layer was thermally grown on the front boron diffusion and then coated with a silicon nitride antireflection layer deposited by PECVD, which may have provided atomic hydrogen to the interface. It took until 1986 to incorporate $SiO_2$ to the surface of phosphorus diffusions, and this permitted to make a 20% efficient $n^+pp^+$ solar cell [24]. The long delay can partly be attributed to the fact that common phosphorus diffused regions had a "dead layer" near the surface, where an excess concentration of electrically inactive dopant atoms caused very fast carrier recombination. The benefits of surface passivation can only be gained once phosphorus precipitates were avoided and the dopant profile optimised [25].

Fig. 6, taken from [26] shows measurements of the recombination current density parameter $J_0$ for phosphorus and boron diffused regions having different dopant doses, as reflected in their respective sheet resistances. Un-passivated, metal-coated diffusions are shown on the left, indicating that the best way to reduce recombination in that case is to use a high dopant dose, either by making the diffusion deep or increasing the surface dopant concentration, or both. On the other hand, for well-passivated diffusions (with PECVD $SiN_x$ for the $n^+$ and ALD $Al_2O_3$ for the $p^+$ surfaces), shown on the right of Fig. 6, it is better to reduce the dopant dose. Doing that permits to keep Auger recombination at bay and achieve $J_0$ values in the range of 10 fA/cm$^2$, or lower. It is interesting to note that, for a given sheet resistance, passivated boron diffusions present a lower $J_0$ than phosphorus diffusions; this can be explained by the fact that the Auger coefficient [27] is lower for for electrons in p-Si, $C_p = 0.99 \times 10^{-31}$ cm$^6$ s$^{-1}$ than for holes in n-Si, $C_n = 2.8 \times 10^{-31}$ cm$^6$ s$^{-1}$. The result may be surprising if one considers that in moderately doped silicon the mobility for holes is smaller than that of electrons, which would mean that a heavier doping is required for p-type Si than n-type Si to achieve the same sheet resistance; nevertheless, this does not apply to high dopant concentrations, for which the difference between electron and hole mobilities is relatively small, both for majority and minority carrier mobilities, as shown in the inset.

When passivating highly doped surfaces, it is important to pay attention to the charge that accompanies some passivating materials. Whereas $SiO_2$ and a-Si:H can be used on any surface, positively charged materials like $Si_3N_4$ and $HfO_2$ are preferable for phosphorus diffusions, and negatively charged ones, like $Al_2O_3$ and $Ga_2O_3$ for boron diffusions. A negative charge onto a phosphorus diffused surface tends to deplete it of electrons and to increase the concentration of holes, hence reducing the asymmetry between both and increasing the recombination rate.

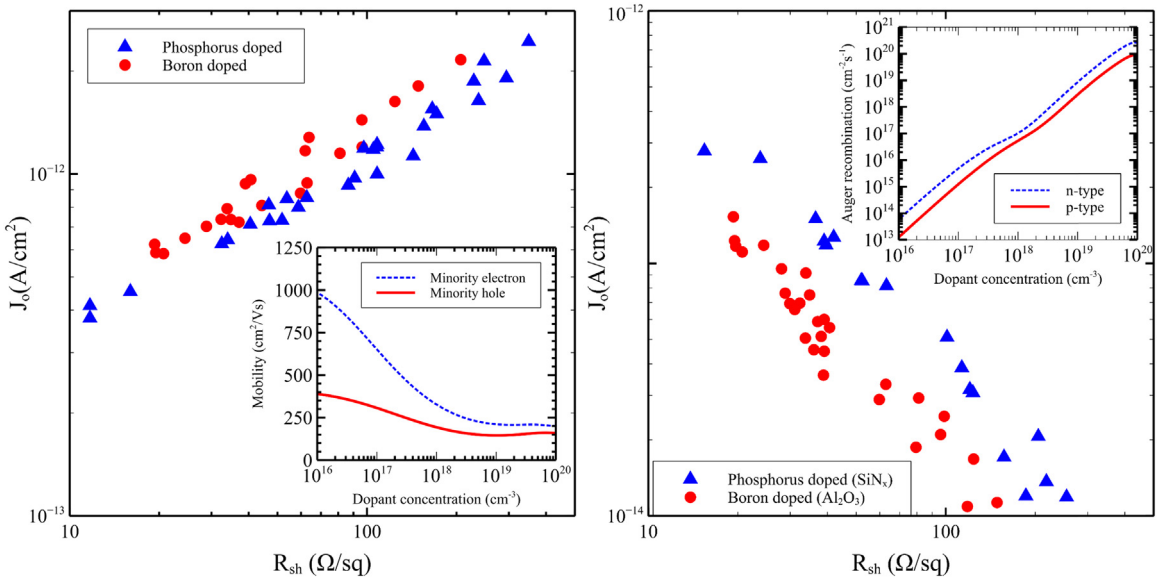


**Fig. 6.** Recombination current density parameter measured for various phosphorus and boron diffused regions having different sheet resistances. Un-passivated, metal-coated diffusions are shown on the left, whereas well-passivated diffusions (with SiNx for phosphorus and Al2O3 for boron diffusions) are shown on the right. The insets show the minority carrier mobilities and Auger recombination rates corresponding to heavily doped n-type or p-type silicon. (From Di Yan, PhD thesis, The Australian National University, 2016).

Table 1 gives experimental values measured for several materials deposited by PECVD or ALD onto typical phosphorus and boron diffused regions having a sheet resistance of about 85–120 Ω/□. The different charge polarity of the dielectric materials is reflected in the difficulty to passivate boron diffusions with $HfO_2$, or phosphorus diffusions with $GaO_x$ and $TiO_x$. To stress the quality of passivation achieved, it is worth noting that some of the measured $J_0 \approx 20–25\ fA/cm^2$ can be almost completely attributed to Auger recombination within the doped layer.

### 3.3. Combining chemical passivation and doping "in series"

One approach to circumvent the poor conductivity of most passivating dielectrics is to make them extremely thin, so that carriers can tunnel through them. The idea, explored in the past for MIS and MINP solar cells, mainly using $SiO_2$, has been extended more recently to other materials. Using Al as the metal, Bullock et al. [28] found that $Al_2O_3$ deposited by ALD onto a phosphorus diffusion gave similar results to a thermally grown $SiO_2$, albeit with poorer stability upon annealing at low temperature. For an optimum $Al_2O_3$ thickness of ~2.2 nm they measured a $J_{0c} \sim 300\ fA\ cm^{-2}$ on a ~100 Ω/□ phosphorus diffusion, together with a low contact resistivity of 0.3 mΩcm$^2$. In subsequent work [29] they achieved a very similar $J_{0c} \sim 300\ fA/cm^2$ with a 1.9 nm $SiO_2$ layer, but a much higher $\rho_c \sim 200\ m\Omega\ cm^2$. Attempts to apply a thin $Al_2O_3$ layer onto boron diffusions failed to produce satisfactory results.

Even though a $J_{0c} \sim 300\ fA\ cm^{-2}$ can be achieved without a thin interlayer under the metal, the dopant diffusion would need to be very deep and with a high dopant dose, as shown in Fig. 6. In contrast, the MIS approach can achieve similar results with a light diffusion, which could be further passivated with $SiN_x$ in the non-contacted areas. This would make it suitable for the front, illuminated side of the solar cell. In such scenario, although the metal contact itself would comprise doping and passivation in series, it would still be applied together with geometrical restriction and placed "in parallel" with the rest of the diffused region.

Selective contacts applied to the back do not need to satisfy the requirement of being transparent (unless the cell is bifacial). With that aim, Bullock et al. [30] developed an enhanced metal-insulator-silicon (MIS) structure based on a lightly diffused $n^+$ region passivated with a $SiO_2$/*a*-Si:H stack, completing the contact formation by means of a thermally-activated alloying process between the *a*-Si:H layer and an overlying aluminium film. The best MIS($n^+$) contacts, with $SiO_2$ thicknesses of ~1.55 nm, achieved a contact resistivity $\rho_c$ of ~3 mΩ cm$^2$ and a recombination current density $J_{0c}$ of ~40 fA/cm$^2$, which remained stable at temperatures up to 350 °C. This selective contact structure was uniformly applied to the rear of n-type silicon solar cells fabricated with a front boron diffusion, achieving a conversion efficiency of 21.0%.

As an alternative to the above contacts, Bullock et al. [31] inserted an intrinsic hydrogenated amorphous silicon passivating film between the dopant-diffused silicon surface and the aluminium electrode. For phosphorus diffusions with a sheet resistance of ~ 110 Ω/□ they achieved $\rho_c \sim 0.05\ \Omega\ cm^2$ and $J_{0c} \sim 40\ fA/cm^2$ for *a*-Si:H(*i*) thicknesses in the 12–15 nm range. Such $J_{0c}$ value was practically the same as that measured for the same $n^+$ diffusion passivated with a PECVD $SiN_x$ layer, and 25 times lower than the value measured when the diffusion was coated with Al. This clearly shows that adding chemical passivation (by a-Si:H in this case) to selective conductivity (from $n^+$ diffusion) can produce excellent passivating contact systems with a contact resistivity sufficiently low for full area applications. A similar experiment on $p^+$ boron diffusions produced $\rho_c \sim 0.1\ \Omega\ cm^2$ and $J_{0c} \sim 200\ fA/cm^2$. Note that the ideal thickness of a passivating interlayer is approximately 10 times greater for a semiconductor like a-Si:H than for a dielectric like $Al_2O_3$.

### 3.4. Burying a dielectric under a doped semiconductor

The combination of a1–2 nm buried $SiO_x$ layer and a 20–200 nm thick phosphorus (or boron) doped silicon film is very effective at suppressing hole (or electron) recombination, and permitting electron (or hole) transport. Among the different methods available, we have used PECVD equipment and silane to deposit an intrinsic amorphous silicon layer (a-Si) and then dope it by conventional phosphorus or boron diffusion from $POCl_3$ or $BBr_3$ [32,33]. Such doping step simultaneously serves to increase the crystallinity of the deposited silicon, and slightly in-diffuse the dopant into the silicon wafer, both of which are critical to achieve good contact and passivation properties. The process to form the interfacial oxide is very simple, either by

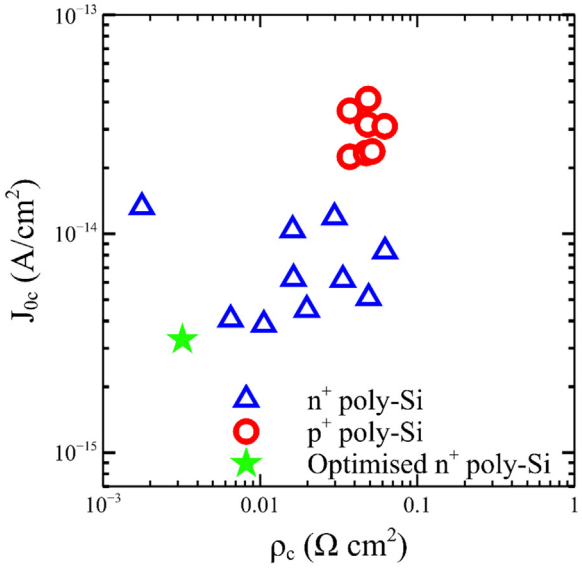


**Fig. 7.** Pairs of contact resistance and recombination current density parameter measured for various polycrystalline silicon/$SiO_x$ passivating contacts formed by chemical vapour deposition and doped by thermal diffusion of either phosphorus or boron. (From Di Yan, PhD thesis, The Australian National University, 2016).

thermal treatment of the wafers in oxygen or by immersing them in hot nitric acid. As shown in Fig. 7, we have found that hole-selective contacts based on $p^+$ polysilicon usually present slightly worse parameters, $J_{0c} \approx 15$ fA/cm$^2$ and $\rho_c \approx 10$ mΩ cm$^2$. Nevertheless, according to Fig. 5, these parameters would still permit to achieve a high conversion efficiency. For the electron-selective contacts we have recently achieved $J_{0c} \approx 3$ fA/cm$^2$ and $\rho_c \approx 4$ mΩ cm$^2$, which applied to the rear side of an n-type silicon solar cell have led to a 24.7% conversion efficiency [34]. In addition to the chemical vapour deposition approach, we have developed a physical deposition technique [35] and used it to form a hole-selective full area passivating contact on the rear of a p-type silicon wafer, achieving a 23.0% solar cell conversion efficiency [36].

The effectiveness of these $SiO_x$/polycrystalline silicon contact structures is probably related, at least in part, to the fact that the doping process causes a "tail" of phosphorus (or boron) into the silicon wafer. Typically, the measured electrically-active dopant profiles show a concentration above $10^{20}$ cm$^{-3}$ in the polycrystalline silicon film followed by an abrupt drop at the location of the thin oxide, down to about $10^{19}$ cm$^{-3}$. The dopant "tail" into the wafer can, therefore, be expected to reduce the concentration of minority carriers at the interface, adding a level of carrier population control to the chemical passivation provided by the $SiO_x$. The physical mechanisms for majority carrier transport and minority carrier blocking are still being debated, and both tunnelling and pinholes in the oxide seem to be able to explain the experimental results. In any case, it is clear that the outstanding results achieved with polysilicon contacts would not be possible without the thin $SiO_x$ layer since, as Fig. 6 shows, ordinary doped regions present a much higher $J_0$ when contacted by a metal. Even compared to the MIS or MINP approaches discussed above, the results achieved by burying the $SiO_x$ layer, rather than placing it onto the diffused region, can only be described as portentous.

### 3.5. Carrier-selective contacts based on extreme work function materials

Some materials can be relatively good conductors at the same time as having an extreme work function. Such combination, together with some level of chemical passivation of the surface, makes them suitable as carrier-selective contacts. A sufficiently high, or low, work function can sustain either accumulation or inversion conditions under one sun illumination and thus maintain regions near the surfaces with highly asymmetric conductivities for electrons and holes. For example, the high work function of $MoO_x$ (about 6 eV) produces an accumulation layer on p-type silicon and an inversion layer on n-type silicon. Bullock et al. [37] measured the sheet resistance of the inversion layer to be $R_{IL} \sim 12$ kΩ/□. For selecting electrons, it is appropriate to use materials like $LiF_x$, which when capped with Al presents a very low work function of ~ 2.8 eV.

In practice, it is difficult to achieve good chemical passivation with the same material that provides an extreme work function. This may be related to the method used to deposit it; for example, $MoO_x$ deposited by evaporation in a vacuum results in some, but insufficient, reduction of surface recombination. Subsequent hydrogenation is difficult, because the material can only be annealed at temperatures below 150 °C. To overcome such difficulties, extreme work-function materials are frequently used in conjunction with a good passivator, like a-Si: H. The risk of inserting an additional layer for chemical passivation is to further hinder the ability to conduct electric current. It is therefore important to simultaneously optimise surface passivation and contact resistance of the complete selective contact structure. Contact resistance usually presents a minimum for very thin interlayers of the extreme work function material, as shown in Fig. 8(a). Nevertheless, this is not a general rule and, for example, the moderate conductivity of $MoO_x$ ($\sim 2 \times 10^{-5}$ S/cm) and $WO_x$ permits a low contact resistivity even with 10–20 nm thick layers, as can be seen in Fig. 8(b). Note that although Pd was used in this instance as the metallic terminal, less extensive tests revealed similar results using evaporated Ni and sputtered indium-tin-oxide (ITO) layers.

Another material that shows promise for hole-selective contacts is copper oxide, which is naturally p-type and has a work function of 4.8–5 eV. Zhang et al. [38] measured a low $\rho_c \approx 11$ mΩ cm$^2$ for an 8 nm thick layer of $CuO_x$:N deposited by sputtering. The layer was identified to contain a mix of $CuO_2$ and CuO, with some nitrogen doping and excess precipitated Cu. More work is, however, required to optimise this material in terms of surface passivation, or combine it with a passivating interlayer.

## 4. Incorporating carrier-selective conductors into solar cells

The ultimate proof that a given material, or a combination of them, can function as a carrier-selective conductor is to apply it to a solar cell. We have done so for a number of them, seeking such a proof-of-concept, with a relatively lower priority given to optimising cell performance. Table 2 summarises the performance of various solar cells fabricated in our laboratory (some steps were performed in some cases at collaborating institutions) using a combination of dopant diffusions, generally at the front side of the device, and a carrier-selective contact system, usually at the rear. For materials that so far have not provided sufficient passivation when deposited directly on silicon we have fabricated solar cells with a partial rear contact, that is, with most of the surface passivated by a conventional material, such as $SiN_x$ for n-type wafers or $Al_2O_3$ for p-type wafers, while the selective conductor itself makes contact on a small fraction, in the range of 1–6%. With some materials ($TaO_x$, $MgO_x$ and $MoO_x$), we attempted a full-area contact, achieving relatively modest open-circuit voltages in the range of 630–640 mV. The benefits of adding an a-Si:H interlayer are clearly demonstrated by the much higher voltages, in the range of 690–710 mV, that can be achieved. An exception is the case of metallic Mg deposited onto the a-Si: H, which seems to have affected the passivation, possibly due to a chemical reaction between the two.

All the cells in the table, except two, were made with n-type silicon wafers, and all the selective conductors, but two, are for electrons. The first hole-selective conductor in the table is $MoO_x$, which we applied directly on 5% of the rear surface of a p-type silicon wafer to replace the customary localised $p^+$ region based on Al or B doping. Thanks to its transparency, $MoO_x$, can also be used at the front side, and the table

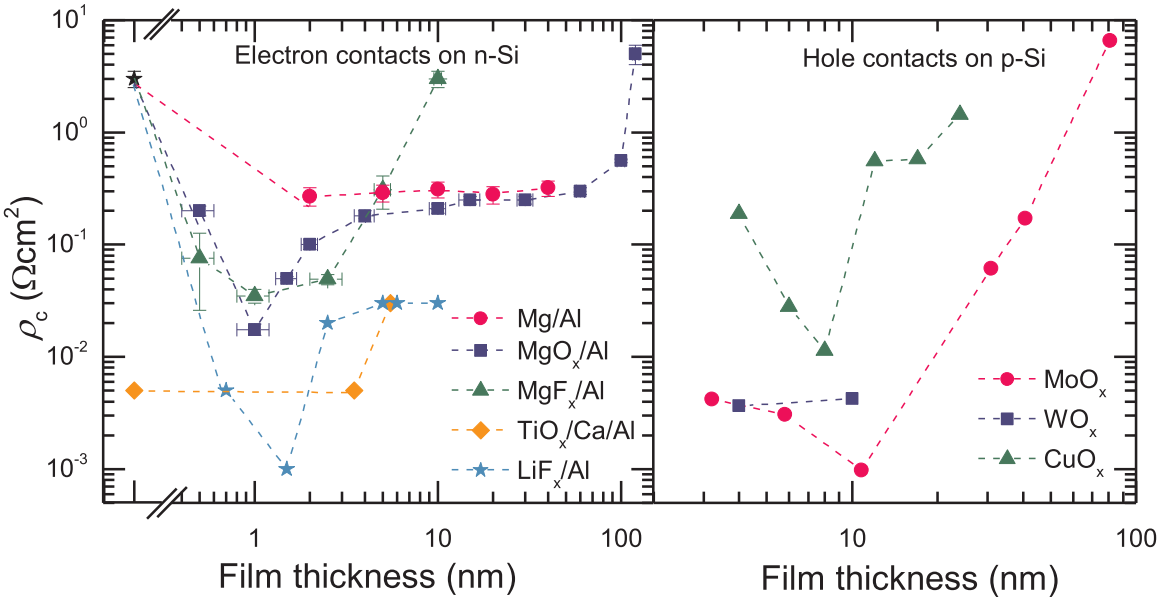


**Fig. 8.** Contact resistivity measurements for various electron-selective and hole-selective contacts as a function of the thickness of the relevant low work-function material. An exception is the case of $TiO_x$/Ca/Al, where the thickness refers to the passivating $TiO_x$ interlayer. In the case of $MoO_x$, $WO_x$ and $CuO_x$ palladium was used as the metal.

shows an example where it was combined with ITO at the front and a phosphorus diffused polysilicon conductor at the rear of an n-type wafer. This device was not optimised, and it did not have a textured surface, which explains its relatively low efficiency of 16.7%. Nevertheless, it proves that a $MoO_x$ conductor does provide a sufficiently low contact resistance on n-type silicon [37].

The table also includes two of the solar cells that we have made recently on both n-type and p-type silicon using a $SiO_x$/polySi conductor for electrons or holes at the rear. The design and fabrication sequence of these devices is considerably more sophisticated than the others in the table. The carrier-selective conductor at the front side was made with two different boron (for the n-type cell) or phosphorus (for the p-type cell) doses, heavier under the metal grid and lighter under the $Al_2O_3/SiN_x$ (just $SiN_x$ for the p-type cell) passivation. The metal bus bar, which surrounds the periphery, does not make contact with the silicon. Thanks to such complexity, it was possible to combine high voltage, current and fill factor, achieving an efficiency of 24.7% with an n-type silicon wafer and 23.0% with a p-type one, which proves the electronic quality of the polysilicon contacts. It can be expected that if a similar level of technological sophistication is used for other selective conductors, higher efficiencies that those reported in the table should be achievable.

## 5. Conclusion

A better understanding of the physics of solar cells has prompted a fresh look at how they can be constructed. Leaving behind deeply entrenched misconceptions, a plethora of previously disregarded materials are being put to good use. Materials that possess a very high work function, like $MoO_x$, or a very low one, like $LiF_x$/Al, which when deposited on silicon create near the surface a thin layer where either electrons or holes are concentrated. That is, a layer that preferentially

**Table 2**
Performance of silicon solar cells that exemplify the various carrier-selective contact systems described in the paper.

| | Selective conductor system | $V_{oc}$ (mV) | $J_{sc}$ (mA/cm$^2$) | FF (%) | Eff. (%) | details | Ref. |
|---|---|---|---|---|---|---|---|
| Partial Rear Contact | $MoO_x$/Ag | 658 | 39.8 | 77.8 | 20.4 | 15 nm $MoO_x$<br>p-Si, 5% contact | Bullock [39] |
| | Ca/Al | 652 | 39.6 | 78.6 | 20.3 | 30 nm Ca<br>n-Si, 1.2% contact | Allen [40] |
| | $TiO_x$/Ca/Al | 681 | 39.6 | 80.9 | 21.8 | 3.5 nm $TiO_x$, 30 nm Ca<br>n-Si, 6.2% contact | Allen [41] |
| | $LiF_x$/Al | 676 | 38.9 | 78.3 | 20.6 | 1.5 nm $LiF_x$<br>n-Si, 1% contact | Bullock [42] |
| Full-area Rear Contact | $MgO_x$/Al | 629 | 39.5 | 80.6 | 20.0 | 1 nm $MgO_x$ | Wan [43] |
| | $TaO_x$/Mg/Al | 638 | 37.8 | 79.3 | 19.1 | 6 nm TaOx<br>10 nm Mg | Wan [44] |
| | a-Si:H/Mg/Al | 637 | 38 | 78.4 | 19.0 | 6 nm a-Si:H,<br>10 nm Mg | Wan [45] |
| | a-Si:H/$MgF_x$/Al | 687 | 37.8 | 77.3 | 20.1 | 6.5 nm a-Si:H,<br>1 nm $MgF_x$ | Wan [46] |
| | $n^+$ c-Si/$SiO_x$/a-Si:H/Al | 666 | 39.3 | 80.5 | 21.0 | 1.5 nm SiOx, Al alloyed to a-Si:H | Bullock [30] |
| | $SiO_x/n^+$ polySi | 705 | 42.4 | 82.6 | 24.7 | n-Si, selective boron diffusion | Yan [34] |
| | $SiO_x/p^+$ polySi | 701 | 41.1 | 79.9 | 23.0 | p-Si, selective phosphorus diff. | Yan [36] |
| Front and rear contact | $MoO_x$/ITO<br>$SiO_x/n^+$ polySi | 637 | 35 | 0.75 | 16.7 | n-Si wafer, not textured | Bullock [47] |
| | a-Si/$MoO_x$/ITO<br>a-Si:H/$TiO_x$/$LiF_x$/Al | 706 | 38.4 | 76 | 20.7 | DASH solar cell | Bullock [48] |

conducts one or the other type of charge carrier. Such selectivity can then be complemented by chemical passivation, that is, by bonding foreign atoms onto the dangling bonds of the silicon surface.

Surface passivation and carrier population control are inextricably linked in the pursuit of two fundamental premises of solar cell operation: to prevent the recombination between carriers and to enable their separate flow towards different terminals. Their combination in what has come to be called “passivating contacts”, which may be applied uniformly across the silicon surface, offers the promise of high performance together with simplicity. Besides being vertically conductive, the materials used in such contact systems need to be transparent, if they are to be applied on the front, illuminated side, or even on the back surface, for bifacial cells. In such applications, the requirement for conductivity is exacerbated by the need to transport current laterally towards the metal grid. Those constraints are very difficult to satisfy with a single material, and all passivating contacts developed so far are composed of multiple layers, each of them performing a specialised function.

The new mentality has led to the development of silicon solar cells that no longer rely on doping for carrier separation. Significant progress has been made in a short period of time, yet there remain many challenges ahead and the journey is still fraught with obstacles. It is uncertain whether or not dopant-less materials and devices will offer advantages for mass production and be stable in the long term. What is clear is that they offer an opportunity to advance scientific understanding and explore new approaches to silicon photovoltaics. Unsurprisingly, the field of passivating selective contacts is expanding rapidly, and is giving silicon solar cell research a renewed impetus.

## Acknowledgement

A significant part of the work presented here has been conducted in collaboration with Ali Javey and co-workers at the University of California at Berkeley (USA), Stefaan De Wolf and co-workers at KAUST (Saudi Arabia), and Christophe Ballif and co-workers at EPFL (Switzerland), the latter also including Stefaan De Wolf before 2016. Josephine McKeon contributed to some of the experimental work at the ANU. We are also indebted to Daniel Macdonald, Sieu Pheng Phang and co-workers at the ANU for synergistic scientific and technological research on silicon solar cells. Funding from the Australian Government via ARENA (project RND003), ACAP (project on "Passivated contacts") and the ARC (DP150104331) is gratefully acknowledged.

## References

[1] A. Cuevas, T. Allen, J. Bullock, W. Yimao, Z.Xinyu. Di, Skin care for healthy silicon solar cells, in: Proceedings of the IEEE 42nd Photovoltaic Specialist Conference (PVSC), 2015, pp. 1–6.
[2] U. Wurfel, A. Cuevas, P. Wurfel, Charge carrier separation in solar cells, IEEE J. Photovolt. 5 (2015) 461–469.
[3] W.D. Eades, Characterization of Silicon-Silicon Dioxide Interface Traps Using Deep Level Transient Spectroscopy (Ph.D. thesis), Stanford University, 1985.
[4] T.-T. Li, Surface Passivation of Crystalline Silicon by Sputtered Aluminium Oxide (Ph.D. thesis), The Australian National University, 2011.
[5] E. Yablonovitch, R.M. Swanson, W.D. Eades, B.R. Weinberger, Electron-hole recombination at the Si-SiO2 interface, Appl. Phys. Lett. 48 (1986) 245–247.
[6] A. Cuevas, The effect of emitter recombination on the effective lifetime of silicon wafers, Sol. Energy Mater Sol. Cells 57 (1999) 277–290.
[7] D.E. Kane, R.M. Swanson, Measurement of the emitter saturation current by a contactless photoconductivity decay method, in: Proceedings of 18th IEEE PVSC, Las Vegas, 1985, pp. 578–585.
[8] P. Würfel, Physics of Solar Cells: From Basic Principles to Advanced Concepts, Wiley, 2009.
[9] T.G. Allen, Y. Wan, A. Cuevas, Silicon surface passivation by gallium oxide capped with silicon nitride, IEEE J. Photovolt. 6 (2016) 900–905.
[10] Y. Wan, K.R. McIntosh, A.F. Thomson, A. Cuevas, Low surface recombination velocity by low-absorption silicon nitride on c-Si, IEEE J. Photovolt. 3 (2013) 554–559.
[11] Y. Wan, D. Yan, J. Bullock, X. Zhang, A. Cuevas, Passivation of c-Si surfaces by sub-nm amorphous silicon capped with silicon nitride, Appl. Phys. Lett. 107 (2015) 231606.
[12] J. Cui, Y. Wan, Y. Cui, Y. Chen, P. Verlinden, A. Cuevas, Highly effective electronic passivation of silicon surfaces by atomic layer deposited hafnium oxide, Appl. Phys. Lett. 110 (2017) 021602.
[13] J. Cui, S.P. Phang, H.C. Sio, Y. Wan, Y. Chen, P. Verlinden, A. Cuevas, Passivation of phosphorus diffused black multi-crystalline silicon by hafnium oxide, Phys. Status Solidi (RRL) – Rapid Res. Lett. 11 (2017) (n/a-n/a).
[14] T.G. Allen, A. Cuevas, Plasma enhanced atomic layer deposition of gallium oxide on crystalline silicon: demonstration of surface passivation and negative interfacial charge, Phys. Status Solidi (RRL) – Rapid Res. Lett. 9 (2015) 220–224.
[15] J. Cui, T. Allen, Y. Wan, J. McKeon, C. Samundsett, D. Yan, X. Zhang, Y. Cui, Y. Chen, P. Verlinden, A. Cuevas, Titanium oxide: a re-emerging optical and passivating material for silicon solar cells, Sol. Energy Mater. Sol. Cells 158 (2016) 115–121.
[16] Y. Wan, J. Bullock, A. Cuevas, Passivation of c-Si surfaces by ALD tantalum oxide capped with PECVD silicon nitride, Sol. Energy Mater. Sol. Cells 142 (2015) 42–46.
[17] Y. Wan, J. Bullock, M. Hettick, Z. Xu, D. Yan, J. Peng, A. Javey, A. Cuevas, Zirconium oxide surface passivation of crystalline silicon, Appl. Phys. Lett. (2018) (Submitted for publication).
[18] R.B.M. Girisch, R.P. Mertens, R.F. DeKeermaecker, Determination of Si-SiO2 interface recombination parameters using a gate-controlled point-junction diode under illumination, IEEE Trans. Electron Dev. 35 (1988) 203–222.
[19] J. Bullock, Advanced Contacts for Crystalline Silicon Solar Cells (Ph.D. thesis), The Australian National University, 2016.
[20] A. Richter, M. Hermle, S.W. Glunz, Reassessment of the limiting efficiency for crystalline silicon solar cells, IEEE J. Photovolt. 3 (2013) 1184–1191.
[21] A. Fell, A free and fast three-dimensional/two-dimensional solar cell simulator featuring conductive boundary and quasi-neutrality approximations, IEEE Trans. Electron Dev. 60 (2013) 733–738.
[22] R. Brendel, R. Peibst, Contact selectivity and efficiency in crystalline silicon photovoltaics, IEEE J. Photovolt. 6 (2016) 1413–1420.
[23] J.G. Fossum, E.L. Burgess, High-efficiency p+-n-n+ back-surface-field silicon solar cells, Appl. Phys. Lett. 33 (1978) 238–240.
[24] A.W. Blakers, M.A. Green, 20% efficieny silicon solar cells, Appl. Phys. Lett. 48 (1986) 215–217.
[25] A. Cuevas, M. Balbuena, Thick-emitter silicon solar cells, in: Proceedings of the Twentieth IEEE Photovoltaic Specialists Conference, 1988, pp. 429–434.
[26] D. Yan, Heavily Doped Carrier-Selective Regions for Silicon Solar Cells (Ph.D. thesis), The Australian National University, 2016.
[27] J. Dziewior, W. Schmid, Auger coefficients for highly doped and highly excited silicon, Appl. Phys. Lett. 31 (1977) 346–348.
[28] J. Bullock, D. Yan, A. Cuevas, Passivation of aluminium–n+ silicon contacts for solar cells by ultrathin Al2O3 and SiO2 dielectric layers, Phys. Status Solidi (RRL) – Rapid Res. Lett. 7 (2013) 946–949.
[29] J. Bullock, D. Yan, A. Cuevas, B. Demaurex, A. Hessler-Wyser, S.D. Wolf, Passivated contacts to $n^+$ and $p^+$ silicon based on amorphous silicon and thin dielectrics, in: Proceedings of the IEEE 40th Photovoltaic Specialist Conference (PVSC), 2014, pp. 3442–3447.
[30] J. Bullock, A. Cuevas, C. Samundsett, D. Yan, J. McKeon, Y. Wan, Simple silicon solar cells featuring an a-Si:H enhanced rear MIS contact, Sol. Energy Mater. Sol. Cells 138 (2015) 22–25.
[31] J. Bullock, D. Yan, Y. Wan, A. Cuevas, B. Demaurex, A. Hessler-Wyser, S. De Wolf, Amorphous silicon passivated contacts for diffused junction silicon solar cells, J. Appl. Phys. 115 (2014).
[32] D. Yan, A. Cuevas, Y. Wan, J. Bullock, Passivating contacts for silicon solar cells based on boron-diffused recrystallized amorphous silicon and thin dielectric interlayers, Sol. Energy Mater. Sol. Cells 152 (2016) 73–79.
[33] D. Yan, A. Cuevas, J. Bullock, Y. Wan, C. Samundsett, Phosphorus-diffused polysilicon contacts for solar cells, Sol. Energy Mater. Sol. Cells 142 (2015) 75–82.
[34] D. Yan, P. Phang, C. Samundsett, Y. Wan, D. Macdonald, A. Cuevas, In preparation, 2018.
[35] D. Yan, A. Cuevas, Solar Cell Fabrication, PCT/AU2017/000260, in, 2017.
[36] D. Yan, A. Cuevas, P. Phang, Y. Wan, D. Macdonald, 23% Efficient p-type crystalline silicon solar cells with hole-selective passivating contacts based on physical vapor deposition of doped silicon silms, submitted to Appl. Phys. Lett, 2018.
[37] J. Bullock, A. Cuevas, T. Allen, C. Battaglia, Molybdenum oxide MoOx: a versatile hole contact for silicon solar cells, Appl. Phys. Lett. 105 (2014) 232109.
[38] X. Zhang, Y. Wan, J. Bullock, T. Allen, A. Cuevas, Low resistance Ohmic contact to p-type crystalline silicon via nitrogen-doped copper oxide films, Appl. Phys. Lett. 109 (2016) 052102.
[39] J. Bullock, C. Samundsett, A. Cuevas, D. Yan, Y. Wan, T. Allen, Proof-of-concept p-type silicon solar cells With molybdenum oxide local rear contacts, IEEE J. Photovolt. 5 (2015) 1591–1594.
[40] T.G. Allen, J. Bullock, P. Zheng, B. Vaughan, M. Barr, Y. Wan, C. Samundsett, D. Walter, A. Javey, A. Cuevas, Calcium contacts to n-type crystalline silicon solar cells, Prog. Photovolt.: Res. Appl. 25 (2017) 636–644.
[41] T.G. Allen, J. Bullock, Q. Jeangros, C. Samundsett, Y. Wan, J. Cui, A. Hessler-Wyser, S. De Wolf, A. Javey, A. Cuevas, A low resistance calcium/reduced titania passivated contact for high efficiency crystalline silicon solar cells, Adv. Energy Mater. 7 (2017) 1602606.
[42] J. Bullock, P. Zheng, Q. Jeangros, M. Tosun, M. Hettick, C.M. Sutter-Fella, Y. Wan, T. Allen, D. Yan, D. Macdonald, S. De Wolf, A. Hessler-Wyser, A. Cuevas, A. Javey, Lithium fluoride based electron contacts for high efficiency n-type crystalline silicon solar cells, Adv. Energy Mater. 6 (2016) (n/a-n/a).
[43] Y. Wan, C. Samundsett, J. Bullock, M. Hettick, T. Allen, D. Yan, J. Peng, Y. Wu, J. Cui, A. Javey, A. Cuevas, Conductive and stable magnesium oxide electron-selective contacts for efficient silicon solar cells, Adv. Energy Mater. 7 (2017) (n/a-n/a).

[44] Y. Wan, S.K. Karuturi, C. Samundsett, J. Bullock, M. Hettick, D. Yan, J. Peng, P.R. Narangari, S. Mokkapati, H.H. Tan, C. Jagadish, A. Javey, A. Cuevas, Tantalum oxide electron-selective heterocontacts for silicon photovoltaics and photoelectrochemical water reduction, ACS Energy Lett. (2017) 125–131.
[45] Y. Wan, C. Samundsett, D. Yan, T. Allen, J. Peng, J. Cui, X. Zhang, J. Bullock, A. Cuevas, A magnesium/amorphous silicon passivating contact for n-type crystalline silicon solar cells, Appl. Phys. Lett. 109 (2016) 113901.
[46] Y. Wan, C. Samundsett, J. Bullock, T. Allen, M. Hettick, D. Yan, P. Zheng, X. Zhang, J. Cui, J. McKeon, A. Javey, A. Cuevas, Magnesium fluoride electron-selective contacts for crystalline silicon solar cells, ACS Appl. Mater. Interfaces 8 (2016) 14671–14677.
[47] J. Bullock, D. Yan, A. Cuevas, Y. Wan, C. Samundsett, n- and p-type silicon solar cells with molybdenum oxide hole contacts, Energy Procedia 77 (2015) 446–450.
[48] J. Bullock, Y. Wan, Z. Xu, S. Essig, M. Hettick, H. Wang, W. Ji, M. Boccard, A. Cuevas, C. Ballif, A. Javey, Stable dopant-free asymmetric heterocontact silicon solar cells with efficiencies above 20%, ACS Energy Lett. (2018) 508–513.